RSC Sustainability

ROYAL SOCIETY OF CHEMISTRY

PAPER

View Article Online
View Journal | View Issue

Cite this: *RSC Sustainability*, 2024, **2**, 2910

Enhancing the H_2 yield from photoreforming of natural lignocellulose feedstock by two-stage thermo-alkaline hydrolysis pretreatment†

Wei Wang,[ac] Zhenyu Jin,[a] Binhai Cheng*[ad] and Ming Zhao *[ab]

The efficiency of hydrogen production from solar water splitting can be substantially increased by adding natural lignocellulosic feedstock as a sacrificial agent in the process. However, the efficiency of the hydrogen yield from photoreforming (PR) natural lignocellulosic feedstock is still far from that of model compounds. In this paper, we report a new pathway for boosting H_2 yield by simply applying a commercial $SrTiO_3$ catalyst in PR processes following thermo-alkaline hydrolysis acidizing (TAH-A), thermo-alkaline hydrolysis reversed-phase (TAH-RP) filtration, and two-stage thermo-alkaline hydrolysis (TS-TAH) pretreatment. The efficiency of the hydrogen yield from PR natural lignocellulosic feedstock was significantly improved through all the pretreatments. The greatest enhancement was found for TS-TAH corn stover, where the hydrogen yield reached 4.7 μmol, which is 2.3 times higher than that of TAH-RP filtration. The advantage was attributed to the elimination of most of the lignin from the corn stover following the TS-TAH. This greatly restrained the light-absorbing effect of lignin from the lignin-TAH-PR system, and more light energy was applied to excite the catalyst for H_2 evolution. This featured finding potentially provides a feasible method for in-depth utilization of natural lignocellulosic feedstocks in PR hydrogen production technology.

Received 22nd March 2024
Accepted 2nd August 2024

DOI: 10.1039/d4su00142g

rsc.li/rscsus

Sustainability spotlight

Hydrogen (H_2) produced from biomass wastes plays an important role in alleviating the energy crisis and improving the quality of the environment. The hydrogen yield can be substantially increased by adding natural lignocellulosic feedstock as a 'sacrificial agent' in the solar water-splitting process. However, its efficiency is still far from that of model compounds. In this work, we propose a new pathway for boosting H_2 yields by simply applying a commercial $SrTiO_3$ catalyst in photoreforming (PR) processes following a two-stage thermo-alkaline hydrolysis (TS-TAH) pretreatment of natural lignocellulosic feedstock. We demonstrated that TS-TAH significantly improved the hydrogen production efficiency. The greatest enhancement was found for the TS-TAH of corn stover, where the hydrogen yield reached 4.7 μmol, which was 5.8 times higher than that of TAH-50 (thermo-alkaline hydrolysis diluted 50 times in our previous study). This featured finding potentially provides a feasible method for in-depth utilization of natural lignocellulosic feedstock in PR hydrogen production technology. Our work emphasizes the importance of the following UN sustainable development goals: affordable and clean energy (SDG 7), and industry, innovation, and infrastructure (SDG 9).

1. Introduction

Solar water-splitting hydrogen technology is limited by poor hydrogen production efficiency factors, and these must be overcome for large-scale application to proceed.[1–3] The addition of sacrificial agents can significantly improve the efficiency of photolytic water hydrogen production.[4–6] The sacrificial agents utilized in the current study, such as TEOA,[7] TEA,[4] and NaI,[8] are costly chemical agents with considerable environmental toxicity. Therefore, it is necessary to find inexpensive and environmentally friendly substitutes for further scaling up of photoreforming (PR) hydrogen production.[9–12]

In 1980, Kawai *et al.*[13] first proposed that carbohydrates (sugar, starch, and lignocellulose) could be used as sacrificial agents to split water for hydrogen production under light using $RuO_2/TiO_2/Pt$ catalysts. During this period, research on photolysis of water for hydrogen production was focused on the development of efficient catalysts, and no attention was paid to the study of using biomass resources as sacrificial agents. It was only in 2014 that Speltini and Wakerley *et al.*[10,14] successively proposed the concept of PR lignocellulosic hydrogen production, which served as a foundation for further research. At

[a]*School of Environment, Tsinghua University, Beijing 100084, China. E-mail: ming.zhao@mail.tsinghua.edu.cn; bhcheng1@mail.ustc.edu.cn; Tel: (+86) 010-62784701*
[b]*Research Institute for Environmental Innovation (Suzhou), Tsinghua, Suzhou 215263, China*
[c]*Huaneng Clean Energy Research Institute, Beijing, 102209, China*
[d]*School of Resources and Environmental Engineering, Hefei University of Technology, Hefei, 230009, China*

† Electronic supplementary information (ESI) available. See DOI: https://doi.org/10.1039/d4su00142g

present, research on PR lignocellulosic hydrogen production technology can be broadly divided into two directions: direct use and use with pretreatment.

The current direct use research is focused on cellulose,[14] hemicellulose,[10] and lignin [15] as model sacrificial agents for the PR process. Lignocellulose derivatives such as cellobiose,[16] hydroxymethylfurfural,[17] xylose,[9] and glucose[18] have also been involved in studies. There are relatively few studies on the direct use of natural lignocellulosic feedstocks, and the main actual feedstocks involved are grass,[15] wood,[18] and newspaper.[10] Although some of the studies utilized natural lignocellulosic feedstocks, the efficiency of their PR of hydrogen is still far from that of model compounds, mainly because of the stability of their epidermal lignocellulose, which is difficult to decompose under heterogeneous reaction conditions, and limits the efficiency of PR hydrogen.[10,15,19,20]

To overcome the challenge of the highly stable state of natural epidermal lignocellulosic feedstock, which is difficult to decompose under heterogeneous reaction conditions, researchers have adopted different pretreatment techniques to break through the limitations. For example, Wakerley *et al.*[10] used a KOH solution with a concentration of 10 M to pretreat lignocellulosic feedstock; Zhang *et al.*[21] used 0.6 M H_2SO_4 for high-temperature acid hydrolysis of lignocellulosic feedstock; Wang *et al.*[22] performed hydrothermal pretreatment of lignocellulose using high temperature and pressure; and Nguyen *et al.*[23] pretreated lignocellulosic feedstock with 10 M NaOH.

It was shown that through pretreatment, the lignocellulosic macromolecular polymer structure was depolymerized, and part of the lignocellulose was dissolved in the hydrolysis solution, which further participated in the photolytic water reaction as a sacrificial agent and enhanced the efficiency of hydrogen production from PR lignocellulose. However, the efficiency of PR hydrogen production from natural lignocellulosic feedstock is still greatly lower as compared to that of model compounds. The thermo-alkaline hydrolysis (TAH) pretreatment described in our previous study[24] enhanced the efficiency of hydrogen production from model compounds (cellulose and hemicellulose). Nevertheless, the PR hydrogen production efficiency for natural lignocellulose feedstock is too low, and this study further addresses this issue.

We report a facile method based on thermo-alkaline hydrolysis acidizing (TAH-A), thermo-alkaline hydrolysis reversed-phase (TAH-RP) filtration, and two-stage thermo-alkaline hydrolysis (TS-TAH) pretreatments of lignocellulosic feedstock. All the pretreatments significantly improved the efficiency of PR H_2 production, even though only a commercial $SrTiO_3$ catalyst was used. This featured finding potentially provides the theoretical basis for in-depth utilization of natural lignocellulosic feedstocks in PR hydrogen production technology.

2. Materials and methods

2.1 Reagents

Dichloromethane, sodium formate, sodium acetate, DL-tartaric acid, anhydrous oxalic acid, $SrTiO_3$, NaOH, hydrochloric acid (36–38%), sodium propionate, and lactic acid were purchased from Titan-Shanghai. H_2PtCl_6 (8 wt% in H_2O) was obtained from Sigma-Aldrich. The resistivity of the deionized water used in the experiments was 17.3–18.2 MΩ cm. The natural lignocellulosic feedstocks were obtained from the agricultural product processing plant at the Huifeng Straw Agricultural Products Processing Co., Ltd, China. Prior to the test, natural lignocellulosic feedstock was sieved to maintain a particle size of less than 2.36 mm. All reagents were used without further purification.

2.2 Equipment

X-ray diffraction (XRD) was carried out using a Bruker D8 (5° min^{-1}, 20–80°). Scanning electron microscopy (SEM) images were recorded using an AG Merlin microscope (Carl Zeiss). Transmission electron microscopy (TEM) was performed using a JEM2100 microscope (Carl Zeiss). Elemental analysis was obtained using an EA (EuroVector). The natural lignocellulosic feedstock components (cellulose, hemicellulose, and lignin) were analysed by the paradigm method using a 2000i fiber analyzer (Ankom). The thermostep thermal difference analyser from Eltra was used for the industrial analysis.

2.3 Thermo-alkaline hydrolysis (TAH)

The TAH method was followed according to a previous report.[24] First, 400 mg of natural lignocellulosic raw material was added to a NaOH solution (50 mL, 2 mol L^{-1}). The resulting solution was stirred for 10 minutes and then transferred to a 100 mL Teflon-lined stainless steel autoclave, and heated at 200 °C for 12 hours. It was then cooled naturally to room temperature, and the reaction solution was called TAH.

2.4 Thermo-alkaline hydrolysis acidizing (TAH-A)

The pH of TAH was adjusted to 0.5–1 using hydrochloric acid (36–38%). After the acidified TAH was centrifuged for 10 min at 8000 rpm, the obtained liquid phase was called TAH-A, and the obtained solid phase was called TAH-AS.

2.5 Thermo-alkaline hydrolysis reversed-phase (TAH-RP) filtration

TAH-A was filtered through a reversed-phase filter column, and the obtained liquid phase was called TAH-RP. Prior to use, the filter columns were activated with methanol and deionized water.

2.6 Two-stage thermo-alkaline hydrolysis (TS-TAH)

First, 400 mg of natural lignocellulose feedstock was added to NaOH solution (50 mL, 2 mol L^{-1}). The resultant solution was stirred for 10 min, and then it was transferred to a 100 mL Teflon-lined stainless-steel autoclave and heated for 30 min at 200 °C. After the reaction, the solution was cooled to room temperature in a water bath and then filtered through a 0.45 μm organic filter membrane. The filtered liquid phase was noted as TS-TAH-30. The separated solid was added to the 50 mL of NaOH (2 mol L^{-1}), stirred well, transferred to a 100 mL Teflon-

lined stainless steel autoclave, and then heated at 200 °C for 12 h. It was then naturally cooled to room temperature, and the reaction liquid was noted as TS-TAH (Fig. 1).

2.7 PR lignocellulose to H_2

PR was executed in a customized reactor (see Fig. S8†) with solar light simulators (370 nm). First, 25 mg catalyst and 5 mL TAH/TAH-A/TAH-RP/TS-TAH was added to a 20 mL transparent photoreactor with a rubber septum lid. The reactor was stirred for 10 min, and then aerated with argon for 30 minutes and sealed. Finally, the reactor was irradiated for 12 h under stirring. The hydrogen yield was calibrated by micro gas chromatography (3000 Micro GC, INFICON, USA) using an external standard method.

2.8 Analysis of organic products

Anion chromatography (HPIC integration, Thermo Fisher, USA, separation column: AS11-HC250 × 4 mm, suppressor: ASRS-300 4 mm) was used for the quantitative analysis of the organic products obtained from pretreatment. A gradient elution was used, and the concentration of the eluent (KOH) was 0.8 mM at 0–15 min, 12 mM at 15–30 min, 38 mM at 30–45 min, 50 mM at 45–50 min, and 0.8 mM at 50–55 min. The temperature of the separation column was 35 °C with a flow rate of 1 mL min^{-1}. Samples were diluted 1000-fold before testing and purified by inductively coupled-reversed phase (IC-RP) column. It should be noted that the adsorption dissociation performance of the chromatography column and the differences between the samples may bias the results, but will not affect the trend of the data. Blank samples were added for analysis between the samples, the eluent (KOH) concentration was set to 30 mM, and the chromatography column was washed for 10 min.

Gas chromatography-mass spectrometry (GC-MS, 7890A-5975C, Agilent, USA, chromatography column: HP-5, carrier gas: He) was used for the qualitative detection of organic products obtained from pretreatment. The initial temperature of the GC column temperature box was 45 °C, which was maintained for 5 min. Then, the column temperature was increased at a rate of 5 °C min^{-1} as the box was heated to 250 °C, and the temperature was maintained for 10 min; the operating temperature of the MS heater was 280 °C. All samples were extracted with ether or dichloromethane prior to testing.

3. Results and discussion

3.1 Characterization of natural lignocellulose feedstock

Compositional analysis of the actual lignocellulosic feedstock was carried out, including lignocellulosic distribution analysis (see Table 1), elemental analysis (see Table S1†), and industrial analysis (see Table S2†). As shown in Table 1, the percentages of cellulose by mass in rice straw, wheat straw, corn straw, soybean straw, and reed straw were similar, while the content in pine was relatively low at 10.33 wt%. The hemicellulose in rice straw, wheat straw, corn straw, and reed straw is greater than 25%, while the content in soybean straw and pine is less than 15%.

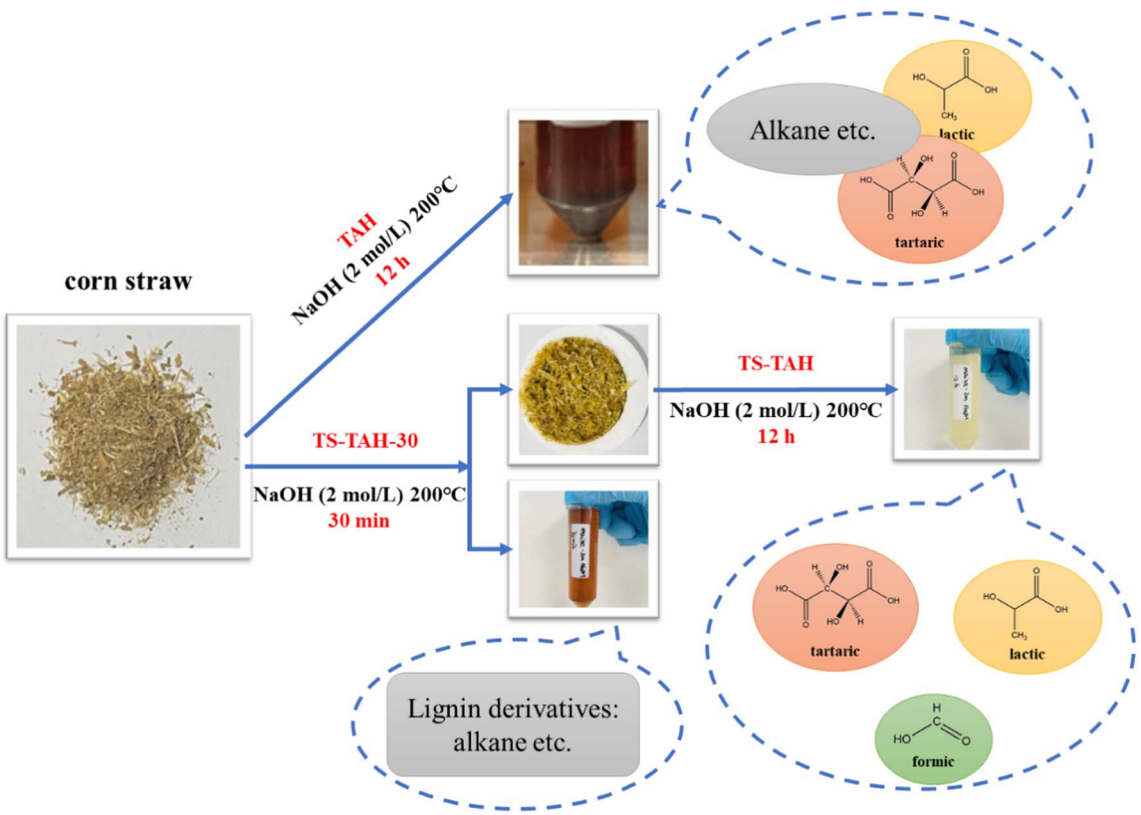

Fig. 1 Two-stage thermo-alkaline hydrolysis (TS-TAH) of corn straw.

Table 1 Constituent analysis of natural lignocellulose feedstock

Sample	Cellulose (wt%)	Hemicellulose (wt%)	Lignin (wt%)
Rice straw	37.81 ± 0.13	27.24 ± 0.21	3.44 ± 0.31
Wheat straw	34.70 ± 1.24	32.14 ± 0.41	6.97 ± 1.29
Corn straw	36.09 ± 0.59	29.35 ± 0.73	3.91 ± 0.83
Soybean straw	31.93 ± 1.46	14.94 ± 0.09	13.54 ± 0.14
Reed straw	35.32 ± 0.96	25.81 ± 1.46	13.26 ± 2.47
Pine	10.33 ± 2.49	8.77 ± 0.28	62.30 ± 2.81

Pine contains approximately 60% lignin, far more than other natural lignocellulosic feedstocks. When the feedstocks were treated with TAH, the polymers, including cellulose, hemicellulose, and lignin, degraded to several types of organic acid. When the main ingredient of certain natural lignocellulosic feedstocks was removed by TAH, the light absorption was weaker and more energy was applied to the liquid phase, which led to more hydrogen production.

Table S1† displays the elemental distribution in natural lignocellulose feedstocks. All six types of natural lignocellulose feedstock were mainly composed of C, H, O, N, S and Si. The percentages of elemental C, H, and O in natural lignocellulose feedstock were similar. Of these natural lignocellulose feedstocks, pine accounted for the largest proportion of the six elements mentioned above, over 96 wt%, mainly because C, H, and O accounted for the largest mass fractions. Pine contained the greatest amount of elemental N, while reed straw contained the least amount. For S, the content in rice straw, wheat straw, maize straw, soybean straw, and reed straw was approximately 0.10 wt%, while pine contained the least at 0.02 wt%. The content of Si varied considerably from sample to sample, with rice straw accounting for the greatest amount at 6.43 wt%, and pine the least at 0.70 wt%.

Table S2† illustrates that the moisture content of the natural lignocellulose feedstock was approximately 7 wt% when stored under sealed conditions at room temperature. In this case, the difference in elemental H and O content may not be due to water content. The ash content varied considerably between the samples, and rice straw contained the largest amount of ash, while the mass fraction of ash in the pine sample was evidently lower than that of the other natural lignocellulose feedstocks. This may explain the difference in elemental C content, because ash mainly consists of inorganic substances, and a feedstock rich in ash such as pine generally contains a low amount of elemental C. The volatile fraction in pine was the largest at 74.68 wt%, while the other samples contained approximately 65 wt%. As for fixed carbon, there was no obvious difference among the natural lignocellulose feedstocks.

3.2 Characterization of the $SrTiO_3$-Pt catalyst

The $SrTiO_3$-Pt catalyst used for the PR process was prepared according to our previous research.[24] The catalysts were characterised, and the results are shown in Fig. S1 and S2.† The blank $SrTiO_3$ and impregnated $SrTiO_3$-Pt samples present typical X-ray diffraction (XRD) patterns of cubic $SrTiO_3$, which matched JCPDS No. 35-0734 (Fig. 2e).[1] Pt was difficult to identify by XRD due to the low loading. The presence of Pt was then confirmed by scanning electron microscopy (SEM), transmission electron microscopy (TEM), and energy dispersive X-ray spectroscopy (EDX).

Fig. 2 shows characterization images of the catalyst used in the research, which proved the existence of Pt. A comparison of the SEM images of $SrTiO_3$ (Fig. 2a) and $SrTiO_3$-0.5Pt (Fig. 2b) revealed Pt nanoparticles on the surface of $SrTiO_3$. The TEM image of $SrTiO_3$-0.5Pt (Fig. 2c) also shows that Pt nanoparticles exist on the catalyst. The EDX spectrum shows that the Pt nanoparticles were evenly distributed on the surface of the catalyst to catalyze the water-splitting reaction.

3.3 Pretreatment of natural lignocellulose feedstock

Fig. 3 demonstrates that total alkali thermal hydrolysis of natural lignocellulosic feedstock was achieved under TAH pretreatment. A small amount of solid appeared at the bottom of the centrifuge tube with the solution left in place, and this occurred because the original sample contained traces of inorganic material that could not be decomposed under TAH. The above tests confirmed that total lignocellulosic hydrolysis could be achieved under TAH for common lignocellulosic feedstocks represented by rice straw, wheat straw, corn straw, soybean straw, reed straw, and pine. The hydrolysis was in general agreement with the model compounds (cellulose, hemicellulose, and lignin) utilised in the previous study.[24] This further suggests that under the TAH conditions mentioned herein, full hydrolysis of cellulose, hemicellulose, and lignin at different ratios can be achieved, even with small amounts of impurities.

Fig. 3 and S1† show the TAH-A and TAH-AS of natural lignocellulosic feedstocks after TAH acidizing. The colour of the TAH-A solutions of natural lignocellulosic feedstock was significantly lighter than that of TAH, mainly because the solubility of the large organic compounds in TAH-A decreased with decreasing alkali concentration (see Tables S3 and S4†). A significant reduction in the solubility of organic matter in TAH occurred when the pH of the solution was less than 1. Complete separation of the dissolved material from TAH-A was achieved by a simple centrifugation process.[25] The TAH-AS was dark brown in colour, and the distribution is shown in Table S4.† The TAH-AS contained mainly benzenes including 1,3-bis(1,1-dimethylethyl)-benzene and 2,4-bis(1,1-dimethylethyl)-phenol. Compared to TAH (see Table S3†), the benzene content in TAH-AS was significantly higher. This indicates that despite the fact that the TAH-A pretreatment facilitates the removal of alkanes, the process may react to produce some amount of benzenes.[20,25] Although most of the alkanes can be removed, a minor amount will remain in the TAH-A. After filtration of TAH-A through the RP column, TAH-RP filtration of all natural lignocellulosic feedstocks resulted in their colour becoming substantially lighter, and changing from yellow to colourless and clear. This indicated that the alkanes and benzenes remaining in TAH-A were further removed.[26,27]

The natural lignocellulosic feedstocks underwent TS-TAH pretreatment, and the solution colour significantly lightened

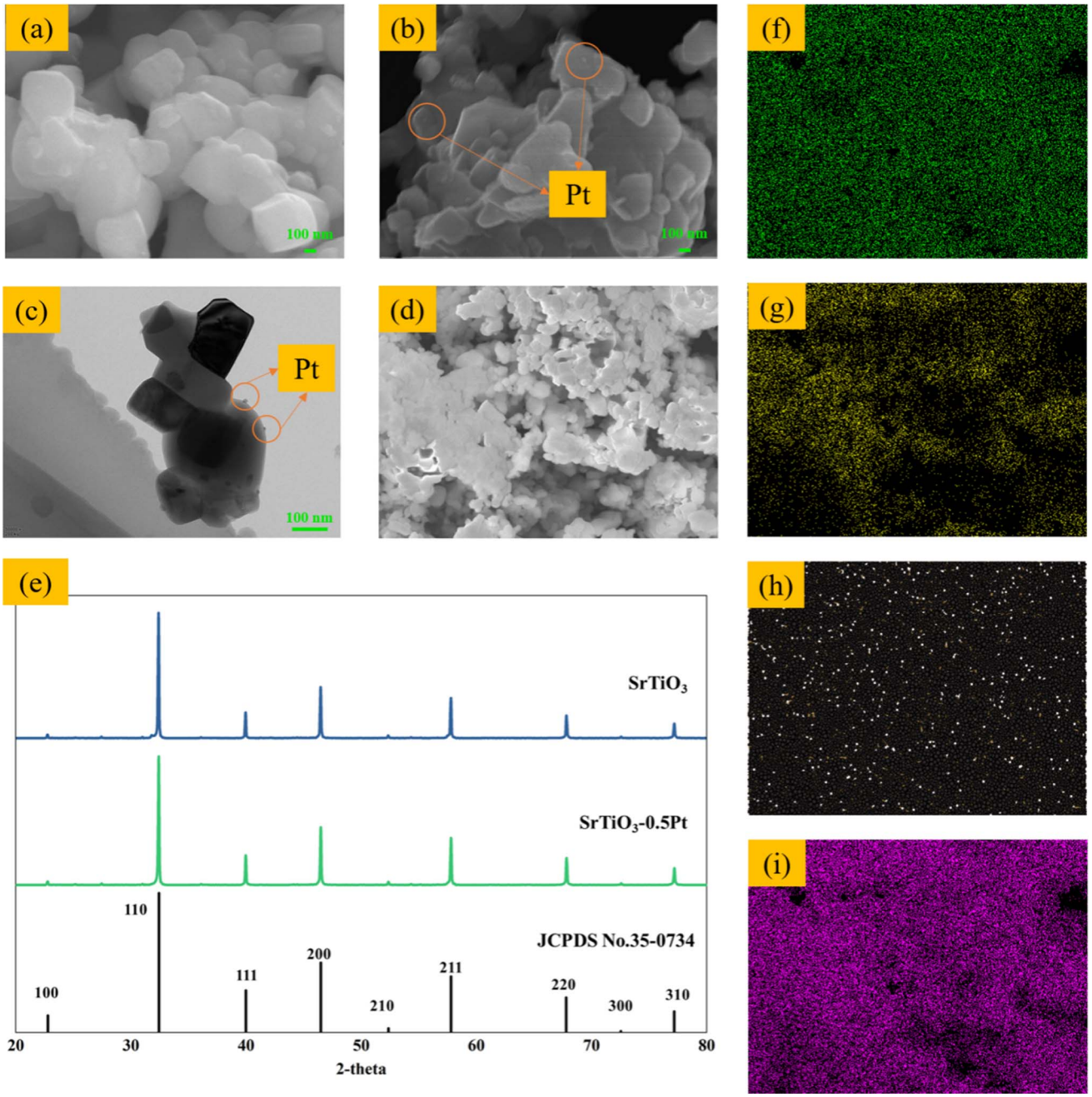

Fig. 2 Characterization of $SrTiO_3$-Pt. (a) SEM image of $SrTiO_3$, (b) SEM image of $SrTiO_3$-0.5Pt, (c) TEM image of $SrTiO_3$-0.5Pt, (d) area scanned by EDS, (e) XRD patterns for the $SrTiO_3$ and $SrTiO_3$-Pt catalysts, (f) EDS image of elemental Ti, (g) EDS image of elemental O, (h) EDS image of elemental Pt, and (i) EDS image of elemental Sr.

from yellowish brown to pale yellow, as compared to the TAH samples. The exception was that soybean straw and pine did not significantly lighten after TS-TAH, and the solution colour remained dark brown. TS-TAH-30 played an important role in this process. A comparison of the product distributions, as shown in Tables S5 and S6,† indicated that the main organic products of TS-TAH-30 were similar to those of TS-TAH, mainly alkanes and phenols, including octane and butylated hydroxytoluene. In particular, rice straw contained a certain amount of 2,4-dimethylhexane, which was different from the 3-ethylhexane contained in TS-TAH, and reed straw contained a certain amount of 2,4-dimethylhexane, which was different from the octane from its TS-TAH. The above data also indicated that effective removal of lignin from the actual lignocellulosic feedstock can be achieved by TS-TAH-30 in the TS-TAH pretreatment. The results also further confirmed that the alkanes and phenols from the TS-TAH were generated at the beginning of the reaction, and as the reaction proceeded, substances including alkanes and phenols were further hydrolysed to organic acids, including lactic acid, formic acid, and tartaric acid.[10,24,28]

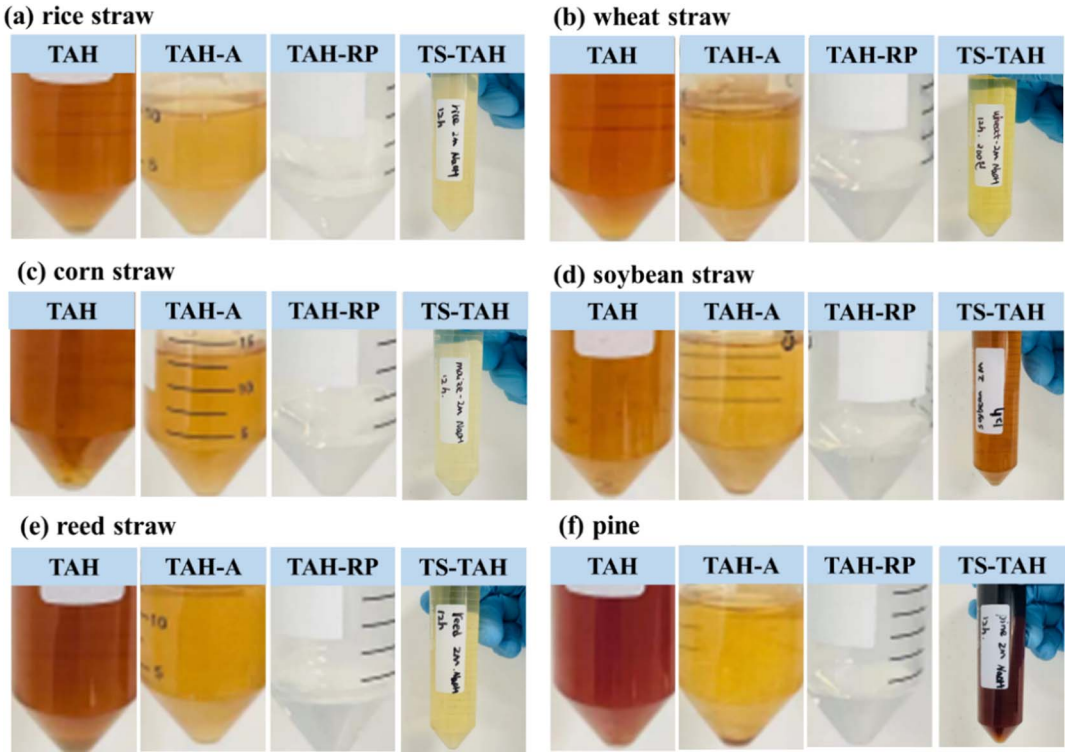

Fig. 3 Comparison of different pretreatment effects of natural lignocellulose feedstock: (a) rice straw, (b) wheat straw, (c) corn straw, (d) soybean straw, (e) reed straw, and (f) pine.

3.4 Organic acid distribution

Organic acids such as lactic, formic, and tartaric acids play a significant role in enhancing the efficiency of hydrogen production from photolytic water.[24,29,30] In this section, the organic acids from TAH and TS-TAH of natural lignocellulosic feedstock were quantified using anion chromatography, and the results are shown in Fig. 4a and 3b, respectively. The total substance content (TSC) derived from the TAH and TS-TAH system of natural lignocellulose feedstocks is fixed at 8000 mg L^{-1} (due to the consistent sample loading of 400 mg in 50 mL). The detected small-molecule acid products *via* IC include: lactic, acetic, propionic, formic, tartaric, and oxalic.

The sum amount of small-molecule acids varied depending on the feedstocks in TAH: 3428 mg L^{-1} for rice straw, 3751 mg L^{-1} for wheat straw, 4374 mg L^{-1} for corn straw, 4450 mg L^{-1} for soybean straw, 5120 mg L^{-1} for reed straw, and 4972 mg L^{-1} for pine. The total acid production from reed straw and pine were higher, accounting for more than 60 wt% of the TSC, and the other straws were approximately 50 wt%. The higher organic acid content from the TAH of reed straw and pine were due to the presence of high levels of lignin in their fractions,[24] and the strong ability of TAH to degrade the cross-linked structure of lignin and consequently promote benzylic acid rearrangement reactions.[31,32] In addition, the yields of tartaric, lactic, and formic acids from TAH were all comparatively higher. The yields of lactic acid and formic acid were comparable, reaching approximately 900 mg L^{-1} and 800 mg L^{-1}, respectively. However, the yields of tartaric acid varied considerably, reaching 3019 mg L^{-1} for pine and only 1202 mg L^{-1} for rice straw.

The sum of the content of small-molecule acids varied depending on the feedstocks in TS-TAH: 1084 mg L^{-1} for rice straw, 1190 mg L^{-1} for wheat straw, 1024 mg L^{-1} for corn straw, 975 mg L^{-1} for soybean straw, 1445 mg L^{-1} for reed straw, and 2079 mg L^{-1} for pine. The total acid production of pine was higher, accounting for 26 wt% of the TSC. Compared to TAH, the acid yield from TS-TAH was significantly lower, mainly since a part of the lignocellulosic feedstock was hydrolysed in TS-TAH-30, causing a decrease in the concentration of the original reactants in TS-TAH. The TS-TAH-30 process removes the lignin from the sample, creating the conditions for its utilisation in the PR of hydrogen production. After TS-TAH, the all-natural lignocellulosic feedstocks contained lactic, acetic, propionic, formic, tartaric, and oxalic acids except for reed straw. This may be caused by the low hemicellulose content of reed straw.[24,33,34] In addition, pine contained more lactic acid, over 400 mg L^{-1}. The yields of acetic acid and tartaric acid were similar across TS-TAH, reaching 120 mg L^{-1} and 130 mg L^{-1}, respectively. The propionic acid yields were both relatively small, below 100 mg L^{-1}. Formic acid yields averaged over 400 mg L^{-1}, with pine wood reaching 583 mg L^{-1}. Oxalic acid yields varied considerably relative to their organic counterparts, reaching 715 mg L^{-1} in pine and only 139 mg L^{-1} in soybean straw. The main reason for this was the large difference in lignin content between the soybean straw and pine, with 62.3 wt% lignin in the pine compared to 13.5 wt% in the soybean straw.[35–38]

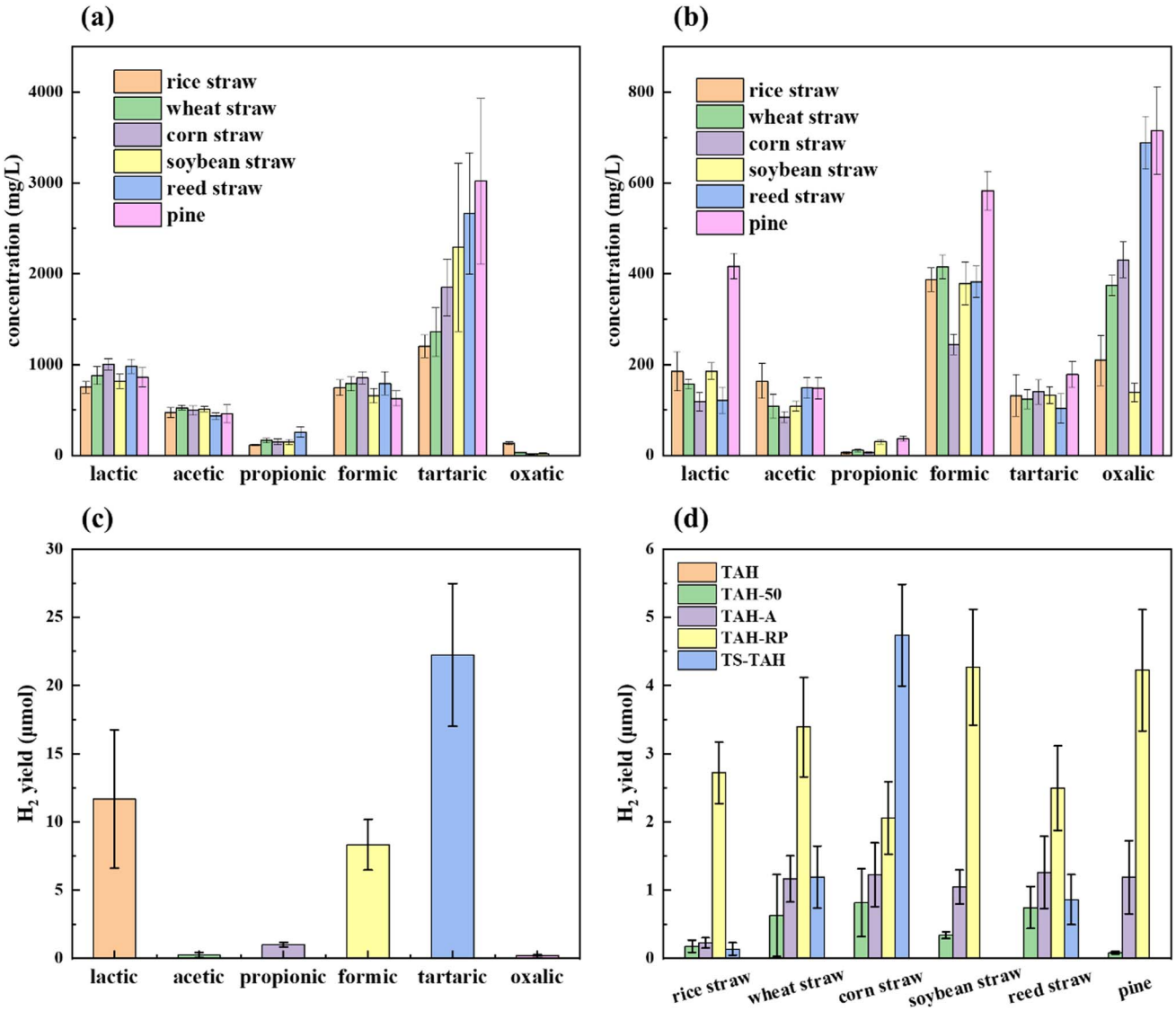

Fig. 4 Organic acid distribution and PR efficiencies. (a) Organic acid distribution of TAH, (b) organic acid distribution of TS-TAH, (c) PR for different single organic acids derived from TAH and TS-TAH using the $SrTiO_3$-Pt catalyst, (d) PR for different TAH solutions using the $SrTiO_3$-Pt catalyst. The error bars represent the standard deviation based on three measured samples. The H_2 yield is the cumulative amount obtained after 12 h.

According to calculations, the elemental C in the small-molecule acid was approximately equal to that of the initial lignocellulosic material. The detailed calculation procedure is shown in the ESI.†

3.5 PR of the natural lignocellulose feedstock

The confirmation experiment with the model compounds in the dark was reported in a previous study, which generated no H_2.[24] The PR efficiencies were in terms of the H_2 yield during 12 h. Fig. 4c illustrates that tartaric acid, lactic acid, and formic acid were the top 3 significant H_2 producers, with H_2 yields of 22, 11, and 8 μmol, respectively. These organic acids were the key factors that enhanced the efficiency of hydrogen production from PR lignocellulosic material (cellulose and hemicellulose), which was demonstrated in our previous study.[24] While lignin also produces the organic acids mentioned above that undergo TAH, the other products from lignin TAH produced strong light absorption, which inhibited their PR hydrogen production efficiency. There was very poor PR hydrogen production from the TAH of natural lignocellulosic feedstocks due to their lignin content.

In this study, the TAH-A, TAH-RP, and TS-TAH pretreatment methods were developed to address the problems of natural lignocellulosic feedstocks undergoing PR for hydrogen production. Fig. 4d compares the effectiveness of the above methods with the previously studied TAH-50 method[24] for boosting the hydrogen production efficiency of PR natural lignocellulosic feedstock. Fig. 4d displays the improvement of hydrogen production efficiency of TS-TAH for different samples, which varied greatly. The greatest enhancement was found for corn stover, where the hydrogen yield reached 4.7 μmol, which

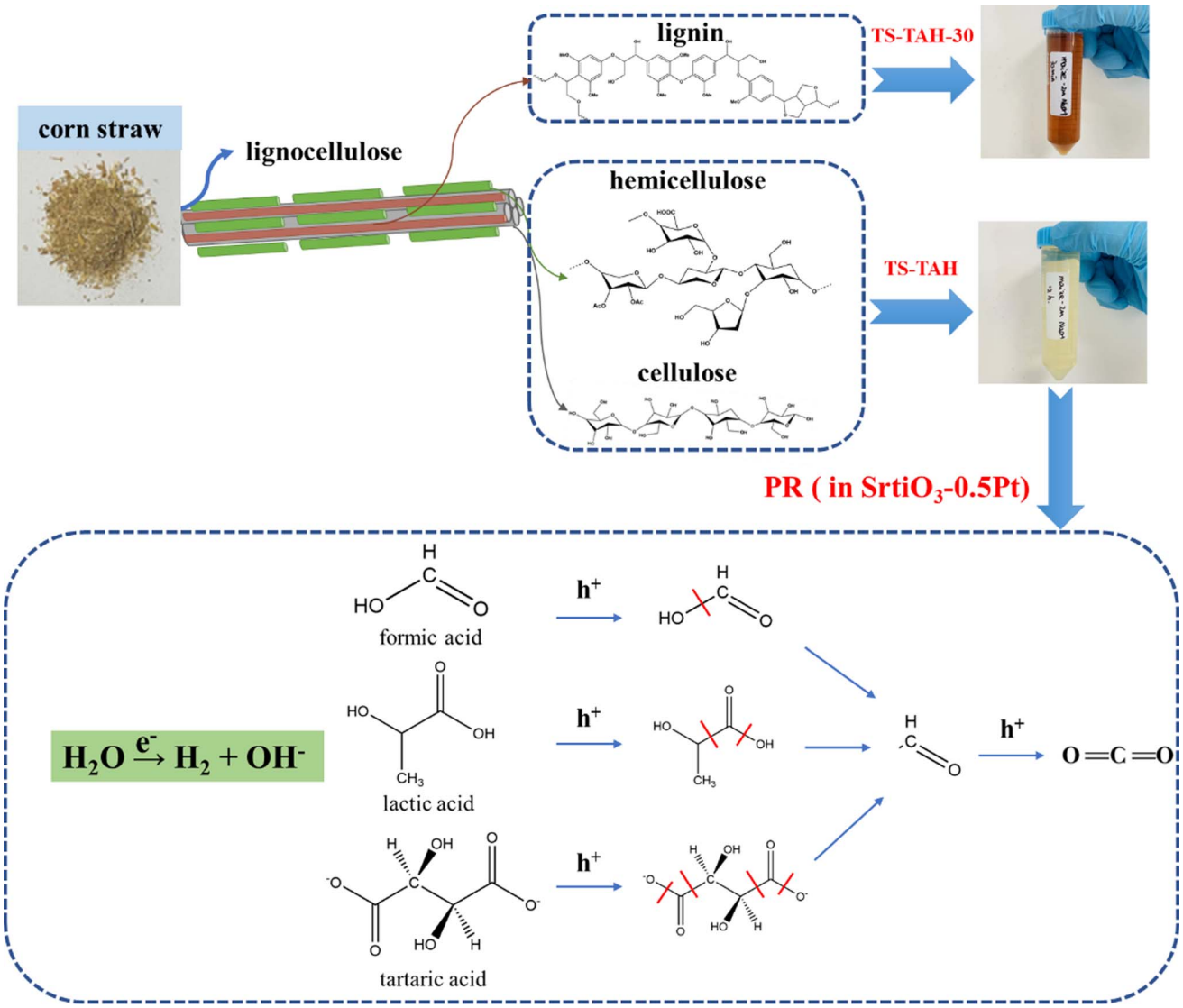

Fig. 5 Reaction pathways of the PR active components of corn straw by TS-TAH.

was 2.3 times higher than that of TAH-RP, and 5.8 times higher than that of TAH-50 (thermo-alkaline hydrolysis with a 50-fold dilution, as performed in our previous study).[24] These results demonstrated that TS-TAH was effective in enhancing the hydrogen production efficiency of PR corn stover, which occurred because the lignin content of corn stover was relatively low compared to the other lignocellulosic feedstocks. Under TS-TAH conditions, the lignin contained in corn stover can be completely removed by TS-TAH-30. Thus, the light absorption of TS-TAH was greatly reduced, and the efficiency of hydrogen production was greatly increased. Ye *et al.*[20] also found that the hydrogen production efficiency of PR corn stover was more advantageous under the same treatment conditions because of the lower lignin content.

TS-TAH of wheat straw also had a certain effect on the improvement of its hydrogen production efficiency. The hydrogen yield reached 1.2 μmol, which was the same as that for TAH-A. TS-TAH of rice straw and reed straw significantly improved the hydrogen production efficiency relative to TAH, and reached the level of TAH-50. However, a large gap remained with TAH-A and TAH-RP. Based on the data in Table 1, the higher lignin content was the main reason for the limited hydrogen production efficiency from the TS-TAH of wheat straw and reed straw. Compared to corn straw, the lignin content of wheat straw and reed straw was two and three times higher than that of corn straw, respectively. Although the lignin content of rice straw was the same as that of corn straw, its structure contained more Si elements, which may produce other organic matter from TS-TAH, thus limiting its hydrogen production efficiency, as detailed in Tables S1, S5, and S6.†

TS-TAH of soybean straw and pine hydrogen production agreed with TAH, and both were without hydrogen generation. This was mainly due to the large amount of lignin in their fractions, with pine reaching 62.3 wt%. With TS-TAH-30, the removal of lignin was limited, resulting in its dark brown colour due to TS-TAH (see Fig. 3). The light absorption from TS-TAH

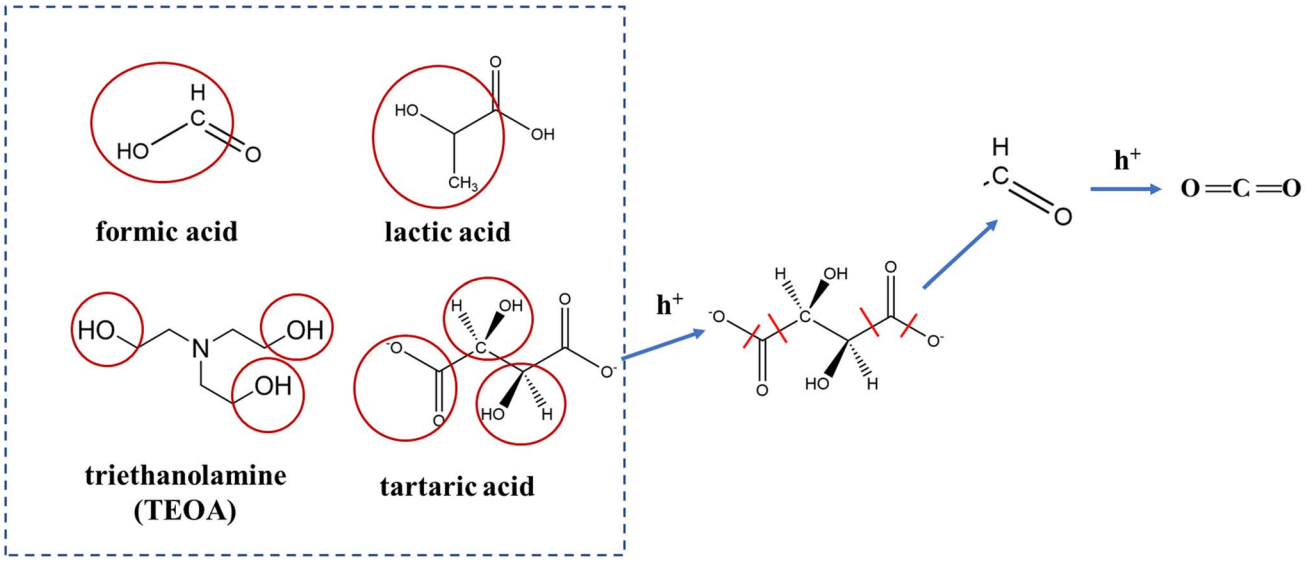

Fig. 6 Mechanism of H_2 production by PR of tartaric acid.

and TAH dominated during the PR reaction. The results in Fig. 4b show that they were ineffective in hydrogen production, although the TS-TAH of soybean straw and pine contained more active components. It further confirmed that the light absorption by large alkanes and benzenes contained in TS-TAH limited the hydrogen production reaction.

3.6 Mechanism of PR lignocellulose based on TS-TAH pretreatment

The above studies confirmed that TS-TAH significantly enhances the efficiency of PR hydrogen from corn stover. It is likely that small-molecule organic acids (tartaric acid, lactic acid, and formic acid) are the key factors that promote hydrogen yield by PR oxidation reactions of lignocellulosic feedstocks based on TAH.[24] Fig. 5 displays a possible rationale for promotion of the hydrogen yield by TS-TAH from the PR of corn stover.

Following the TS-TAH-30 treatment, the vast majority of lignin was eliminated from the corn stover, but a minor amount of residue was contained in the solid phase. Cellulose and hemicellulose produce little oxalic acid during TAH,[24] but the presence of oxalic acid in corn stover after TS-TAH supports the absence of lignin. It greatly restrained the light-absorbing effect from the lignin-TAH-PR system for H_2 evolution.[10,24] Subsequently, TS-TAH hydrolyzed all of the remaining solid phase to the liquid phase. The active components (tartaric acid, lactic acid, and formic acid) in the liquid phase were oxidized by photo-generated holes, and produced aldehyde and formate through C–C bond cleavage, which can be further oxidized to a carboxylic acid and CO_2. Photogenerated electrons reduced water with active component formation of H_2 and hydroxide.

The contribution of organic acids to hydrogen yield in the TS-TAH of corn stover is estimated in Table S7.† Compared to the hydrogen yield from corn stover after TS-TAH, the estimated data were in the same order of magnitude as the actual yield, which indicates that the estimated results are reliable. Therefore, the data illustrate that tartaric acid, formic acid, and lactic acid were the key factors contributing to the increased hydrogen yield in the TS-TAH of corn stover. Due to the complexity of the test process, the condition boundary of the simulation estimation cannot be fully considered. Thus, some deviation resulted between the estimated results and the actual results. However, in combination with the existing studies, the key role of the organic acid in the enhancement of hydrogen yield cannot be denied.

Fig. 6 further shows the PR reaction paths of the active components (tartaric acid, lactic acid, and formic acid). A comparison with the molecular structure of TEOA, the more widely used sacrificial agent in previous studies of photolytic water,[39–41] revealed that all three acids share this advantage, probably because their compounds contain hydroxymethyl (–HC–OH) groups that can simply be oxidized to methylene aldehyde groups, and then further oxidized to CO_2. However, when compared to each other, the production of H_2 by tartaric acid was clearly the greatest among the three (Fig. 4c). This is because tartaric acid contains more hydroxymethyl groups, and is therefore more easily oxidized.

4. Conclusions

TAH-A, TAH-RP, and TS-TAH pretreatment methods were developed to enhance the hydrogen production efficiency of PR natural lignocellulosic feedstocks. TAH-RP significantly improved the hydrogen production efficiency of PR all the feedstocks, and the greatest enhancement was found for TS-TAH corn stover rather than TAH-RP. Future investigations should focus on enhancing the adaptability of TS-TAH to different natural lignocellulosic feedstocks.

Data availability

The data supporting this article have been included as part of the ESI.†

Conflicts of interest

There are no conflicts to declare.

Acknowledgements

This work was supported by the National Key Research and Development Program of China (2019YFC1903902) and Huaneng Clean Energy Technology Research Institute (Grant No. TL-23-CERI02).

References

1 L. C. Mu, Y. Zhao, A. L. Li, S. Y. Wang, Z. L. Wang, J. X. Yang, Y. Wang, T. F. Liu, R. T. Chen, J. Zhu, F. T. Fan, R. G. Li and C. Li, Enhancing charge separation on high symmetry $SrTiO_3$ exposed with anisotropic facets for photocatalytic water splitting, *Energy Environ. Sci.*, 2016, **9**(7), 2463–2469, DOI: 10.1039/c6ee00526h.

2 F. P. G. de Arquer, D. V. Talapin, V. I. Klimov, Y. Arakawa, M. Bayer and E. H. Sargent, Semiconductor quantum dots: Technological progress and future challenges, *Science*, 2021, **373**(6555), 640, DOI: 10.1126/science.aaz8541.

3 P. Raizada, S. Sharma, A. Kumar, P. Singh, A. A. Parwaz Khan and A. M. Asiri, Performance improvement strategies of $CuWO_4$ photocatalyst for hydrogen generation and pollutant degradation, *J. Environ. Chem. Eng.*, 2020, **8**(5), 104230, DOI: 10.1016/j.jece.2020.104230.

4 S. Yanagida, T. Azuma and H. Sakurai, Photocatalytic hydrogen evolution from water using zinc-sulfide and sacrificial electron-donors, *Chem. Lett.*, 1982, (7), 1069–1070, DOI: 10.1246/cl.1982.1069.

5 S. C. Moon, H. Mametsuka, S. Tabata and E. Suzuki, Photocatalytic production of hydrogen from water using TiO_2 and B/TiO_2, *Catal. Today*, 2000, **58**(2–3), 125–132, DOI: 10.1016/s0920-5861(00)00247-9.

6 A. Galinska and J. Walendziewski, Photocatalytic water splitting over Pt-TiO_2 in the presence of sacrificial reagents, *Energy Fuels*, 2005, **19**(3), 1143–1147, DOI: 10.1021/ef0400619.

7 R. Abe, K. Hara, K. Sayama, K. Domen and H. Arakawa, Steady hydrogen evolution from water on Eosin Y-fixed TiO_2 photocatalyst using a silane-coupling reagent under visible light irradiation, *J. Photochem. Photobiol., A*, 2000, **137**(1), 63–69, DOI: 10.1016/s1010-6030(00)00351-8.

8 R. Abe, K. Sayama and H. Sugihara, Development of new photocatalytic water splitting into H_2 and O_2 using two different semiconductor photocatalysts and a shuttle redox mediator IO_3^-/I, *J. Phys. Chem. B*, 2005, **109**(33), 16052–16061, DOI: 10.1021/jp052848l.

9 Q. Liu, L. L. Wei, Q. Y. Xi, Y. Q. Lei and F. X. Wang, Edge functionalization of terminal amino group in carbon nitride by in-situ C-N coupling for photoreforming of biomass into H_2, *Chem. Eng. J.*, 2020, **383**, 1–9, DOI: 10.1016/j.cej.2019.123792.

10 D. W. Wakerley, M. F. Kuehnel, K. L. Orchard, K. H. Ly, T. E. Rosser and E. Reisner, Solar-driven reforming of lignocellulose to H_2 with a CdS/CdOx photocatalyst, *Nat. Energy*, 2017, **2**(4), 1–9, DOI: 10.1038/nenergy.2017.21.

11 Z. Liu, K. Liu, R. Sun and J. Ma, Biorefinery-assisted ultra-high hydrogen evolution via metal-free black phosphorus sensitized carbon nitride photocatalysis, *Chem. Eng. J.*, 2022, **446**, 137128, DOI: 10.1016/j.cej.2022.137128.

12 H. Wang, H. Jiang, P. Huo, M. Filip Edelmannová, L. Čapek and K. Kočí, Hydrogen production from methanol-water mixture over NiO/TiO_2 nanorods structure photocatalysts, *J. Environ. Chem. Eng.*, 2022, **10**(1), 106908, DOI: 10.1016/j.jece.2021.106908.

13 T. Kawai and T. Sakata, Conversion of carbohydrate into hydrogen fuel by a photocatalytic process, *Nature*, 1980, **286**(5772), 474–476, DOI: 10.1038/286474a0.

14 A. Speltini, M. Sturini, D. Dondi, E. Annovazzi, F. Maraschi, V. Caratto, A. Profumo and A. Buttafava, Sunlight-promoted photocatalytic hydrogen gas evolution from water-suspended cellulose: a systematic study, *Photochem. Photobiol. Sci.*, 2014, **13**(10), 1410–1419, DOI: 10.1039/c4pp00128a.

15 H. Nagakawa and M. Nagata, Photoreforming of Lignocellulosic Biomass into Hydrogen under Sunlight in the Presence of Thermally Radiative CdS/SiC Composite Photocatalyst, *ACS Appl. Energy Mater.*, 2021, **4**(2), 1059–1062, DOI: 10.1021/acsaem.0c02530.

16 H. Kasap, D. S. Achilleos, A. Huang and E. Reisner, Photoreforming of Lignocellulose into H_2 Using Nanoengineered Carbon Nitride under Benign Conditions, *J. Am. Chem. Soc.*, 2018, **140**(37), 11604–11607, DOI: 10.1021/jacs.8b07853.

17 V. R. Battula, A. Jaryal and K. Kailasam, Visible light-driven simultaneous H_2 production by water splitting coupled with selective oxidation of HMF to DFF catalyzed by porous carbon nitride, *J. Mater. Chem. A*, 2019, **7**(10), 5643–5649, DOI: 10.1039/c8ta10926e.

18 H. Nagakawa and M. Nagata, Highly Efficient Hydrogen Production in the Photoreforming of Lignocellulosic Biomass Catalyzed by Cu,In-Doped ZnS Derived from ZIF-8, *Adv. Mater. Interfaces*, 2022, **9**(2), 2101581, DOI: 10.1002/admi.202101581.

19 T. Sakata and T. Kawai, Photodecomposition of Water by Using Organic Compounds, *J. Synth. Org. Chem.*, 1981, **39**(7), 589–602.

20 Y. L. Zhou, X. Y. Ye and D. Y. Lin, Enhance photocatalytic hydrogen evolution by using alkaline pretreated corn stover as a sacrificial agent, *Int. J. Energy Res.*, 2020, **44**(6), 4616–4628, DOI: 10.1002/er.5242.

21 J. Zou, G. Zhang and X. X. Xu, One-pot photoreforming of cellulosic biomass waste to hydrogen by merging photocatalysis with acid hydrolysis, *Appl. Catal., A*, 2018, **563**, 73–79, DOI: 10.1016/j.apcata.2018.06.030.

22 M. Wang, M. J. Liu, J. M. Lu and F. Wang, Photo splitting of bio-polyols and sugars to methanol and syngas, *Nat. Commun.*, 2020, **11**(1), 1–9, DOI: 10.1038/s41467-020-14915-8.

23 V. C. Nguyen, D. B. Nimbalkar, L. D. Nam, Y. L. Lee and H. S. Teng, Photocatalytic Cellulose Reforming for H_2 and

Formate Production by Using Graphene Oxide-Dot Catalysts, *ACS Catal.*, 2021, **11**(9), 4955–4967, DOI: 10.1021/acscatal.1c00217.

24 W. Wang, B. Cheng, M. Zhao, E. Anthony, R. Luque and D. D. Dionysiou, Boosting H_2 yield from photoreforming of lignocellulose by thermo-alkaline hydrolysis with selective generation of a key intermediate product: Tartaric acid, *Energy Convers. Manage.*, 2022, **257**, 115444, DOI: 10.1016/j.enconman.2022.115444.

25 S. M. Kang, X. L. Li, J. Fan and J. Chang, Classified Separation of Lignin Hydrothermal Liquefied Products, *Ind. Eng. Chem. Res.*, 2011, **50**(19), 11288–11296, DOI: 10.1021/ie2011356.

26 S. D. Yin, A. K. Mehrotra and Z. C. Tan, Alkaline hydrothermal conversion of cellulose to bio-oil: Influence of alkalinity on reaction pathway change, *Bioresour. Technol.*, 2011, **102**(11), 6605–6610, DOI: 10.1016/j.biortech.2011.03.069.

27 S. D. Yin and Z. C. Tan, Hydrothermal liquefaction of cellulose to bio-oil under acidic, neutral and alkaline conditions, *Appl. Energy*, 2012, **92**, 234–239, DOI: 10.1016/j.apenergy.2011.10.041.

28 H. B. Huang, K. Yu, J. T. Wang, J. R. Zhou, H. F. Li, J. Lu and R. Cao, Controlled growth of ZnS/ZnO heterojunctions on porous biomass carbons via one-step carbothermal reduction enables visible-light-driven photocatalytic H_2 production, *Inorg. Chem. Front.*, 2019, **6**(8), 2035–2042, DOI: 10.1039/c9qi00454h.

29 W. Zhang, Y. B. Wang, Z. Wang, Z. Y. Zhong and R. Xu, Highly efficient and noble metal-free NiS/CdS photocatalysts for H_2 evolution from lactic acid sacrificial solution under visible light, *Chem. Commun.*, 2010, **46**(40), 7631–7633, DOI: 10.1039/c0cc01562h.

30 J. L. Santos, C. Megias-Sayago, S. Ivanova, M. A. Centeno and J. A. Odriozola, Functionalized biochars as supports for Pd/C catalysts for efficient hydrogen production from formic acid, *Appl. Catal., B*, 2021, **282**, 119615, DOI: 10.1016/j.apcatb.2020.119615.

31 H. Peng, Y. Sun, J. H. Zhang and L. Lin, Degradation of cellooligosaccharides in oxidative medium and alkaline medium: HPLC, FTIR, and GC-MS analyses, *BioResources*, 2010, **5**(2), 616–633.

32 Y. Wan and J. M. Lee, Toward value-added dicarboxylic acids from biomass derivatives via thermocatalytic conversion, *ACS Catal.*, 2021, **11**(5), 2524–2560, DOI: 10.1021/acscatal.0c05419.

33 B. Godin, F. Ghysel, R. Agneessens, T. Schmit, S. Gofflot, S. Lamaudiere, G. Sinnaeve, J. P. Goffart, P. A. Gerin, D. Stilmant and J. Delcarte, Cellulose, hemicelluloses, lignin, and ash contents in various lignocellulosic crops for second generation bioethanol production, *Biotechnol. Agron. Soc. Environ.*, 2010, **14**, 549–560.

34 S. S. Dalli, T. J. Tilaye and S. K. Rakshit, Conversion of Wood-Based Hemicellulose Prehydrolysate into Succinic Acid Using a Heterogeneous Acid Catalyst in a Biphasic System, *Ind. Eng. Chem. Res.*, 2017, **56**(38), 10582–10590, DOI: 10.1021/acs.iecr.7b01708.

35 N. C. Luo, T. Montini, J. Zhang, P. Fornasiero, E. Fonda, T. T. Hou, W. Nie, J. M. Lu, J. X. Liu, M. Heggen, L. Lin, C. T. Ma, M. Wang, F. T. Fan, S. Y. Jin and F. Wang, Visible-light-driven coproduction of diesel precursors and hydrogen from lignocellulose-derived methylfurans, *Nat. Energy*, 2019, **4**(7), 575–584, DOI: 10.1038/s41560-019-0403-5.

36 C. Rao, M. L. Xie, S. C. Liu, R. L. Chen, H. Su, L. Zhou, Y. X. Pang, H. M. Lou and X. Q. Qiu, Visible Light-Driven Reforming of Lignocellulose into H_2 by Intrinsic Monolayer Carbon Nitride, *ACS Appl. Mater. Interfaces*, 2021, **13**(37), 44243–44253, DOI: 10.1021/acsami.1c10842.

37 C. H. Li, H. M. Wang, S. B. Naghadeh, J. Z. Zhang and P. F. Fang, Visible light driven hydrogen evolution by photocatalytic reforming of lignin and lactic acid using one-dimensional NiS/CdS nanostructures, *Appl. Catal., B*, 2018, **227**, 229–239, DOI: 10.1016/j.apcatb.2018.01.038.

38 N. Srisasiwimon, S. Chuangchote, N. Laosiripojana and T. Sagawa, TiO_2/Lignin-Based Carbon Composited Photocatalysts for Enhanced Photocatalytic Conversion of Lignin to High Value Chemicals, *ACS Sustainable Chem. Eng.*, 2018, **6**(11), 13968–13976, DOI: 10.1021/acssuschemeng.8b02353.

39 D. Zhao, Y. Wang, C.-L. Dong, Y.-C. Huang, J. Chen, F. Xue, S. Shen and L. Guo, Boron-doped nitrogen-deficient carbon nitride-based Z-scheme heterostructures for photocatalytic overall water splitting, *Nat. Energy*, 2021, **6**, 388–397, DOI: 10.1038/s41560-021-00795-9.

40 M. Yoo, Y.-S. Yu, H. Ha, S. Lee, J.-S. Choi, S. Oh, E. Kang, H. Choi, H. An, K.-S. Lee, J. Y. Park, R. Celestre, M. A. Marcus, K. Nowrouzi, D. Taube, D. A. Shapiro, W. Jung, C. Kim and H. Y. Kim, A tailored oxide interface creates dense Pt single-atom catalysts with high catalytic activity, *Energy Environ. Sci.*, 2020, **13**, 1231–1239, DOI: 10.1039/C9EE03492G.

41 S. S. Chen, Y. Qi, T. Hisatomi, Q. Ding, T. Asai, Z. Li, S. S. K. Ma, F. X. Zhang, K. Domen and C. Li, Efficient Visible-Light-Driven Z-Scheme Overall Water Splitting Using a $MgTa_2O_6$-xNy/TaON Heterostructure Photocatalyst for H_2 Evolution, *Angew. Chem., Int. Ed.*, 2015, **54**(29), 8498–8501, DOI: 10.1002/anie.201502686.